



Cite this: *Environ. Sci.: Water Res. Technol.*, 2018, **4**, 1979

## Exploration of the treatment of fish-canning industry effluents by aqueous-phase reforming using Pt/C catalysts†

A. S. Oliveira, J. A. Baeza, L. Calvo, \* N. Alonso-Morales, F. Heras, J. Lemus, J. J. Rodriguez and M. A. Gilarranz

In the current work, an exploratory study on the application of catalytic aqueous phase reforming (APR) to the treatment of fish-canning wastewater was performed for the first time. Pt/C (3%, w) catalysts were supported on different commercial carbon supports (two activated carbons and a carbon black) and tested in the APR of tuna-cooking wastewater. The effect of the supports and the reaction systems (batch vs. semi-continuous) on the performance of the catalysts was tested. The stability of the catalysts upon 3 successive reuse cycles was checked. TOC and COD removal ranged within 45–60%, which was ascribed to adsorption on the supports, hydrothermal carbonization and APR. The percentage of valuable gases (H<sub>2</sub> and alkanes) reached up to 18% of the gas production showing the potential of APR for the valorization and treatment of wastewater. The production of gases is affected by the high chloride, acetate and phosphate concentrations, which may provoke catalyst deactivation. The use of a catalyst with a basic support significantly increased the production of gases and the H<sub>2</sub> percentage in the gas fraction. Gas production was higher in semi-continuous compared to batch operation, maybe because the withdrawn gas displaces the reaction towards the products. The percentage of alkanes in the gas phase decreased upon successive catalyst reuse cycles at the expense of H<sub>2</sub>, which is probably due to sintering of Pt nanoparticles with the corresponding decrease of the number of low-coordinated Pt sites promoting methanation reactions.

Received 20th June 2018,  
Accepted 12th September 2018

DOI: 10.1039/c8ew00414e

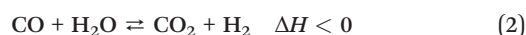
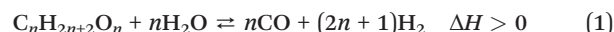
rsc.li/es-water

### Water impact

The research presented in our manuscript relates to the aims and scope of the journal since it shows for the first time the application of catalytic aqueous phase reforming for the treatment of wastewater. The main objective of this work is not only to remove the organic load in wastewater, but also to assess whether the energy from the gases produced can compensate for the inputs. Moreover, it is the first application of the aqueous phase reforming for the valorization and treatment of wastewater from the food industry, which has been scarcely studied in the literature.

## 1. Introduction

Aqueous-phase reforming (APR) has gained much attraction since the pioneering work by Cortright *et al.* (2002).<sup>1</sup> In that work, the possibility of obtaining valuable gases from oxygenated hydrocarbons in water, which can be found in renewable sources such as biomass waste streams, was shown. The main reactions involved in the APR process to form H<sub>2</sub> are reforming (eqn (1)) and water-gas shift reaction (eqn (2)), but methanation and Fischer–Tropsch reactions consuming H<sub>2</sub> to form alkanes can also take place.<sup>1</sup>



Since then, great efforts have been made, mostly focused on the APR of model compounds such as glucose, sorbitol, xylitol, galactitol, ethanol, 1-propanol, glycerol and ethylene glycol, among others.<sup>2–11</sup> In most of these studies, the main objective was to determine the effect of the catalysts and the operating conditions, in order to drive the process towards a high yield of valuable gases. In particular, studies on APR of glycerol have gathered growing interest since it is the main by-product from biodiesel production highly available in aqueous streams from biorefineries.<sup>5,11–14</sup>

According to the promising results reported from the APR of all the above compounds in terms of conversion and

Departamento de Ingeniería Química, C/Francisco Tomás y Valiente 7, Universidad Autónoma de Madrid, 28049 Madrid, Spain.

E-mail: luisa.calvo@uam.es

† Electronic supplementary information (ESI) available. See DOI: 10.1039/c8ew00414e



selectivity to  $H_2$ , the process could be extended to new potential applications, such as the treatment of biomass-bearing wastewater. Since APR requires the use of catalysts, temperatures around 200–250 °C and pressures between 15 and 50 bar, the success of this application and its real competitiveness with traditional treatments would be also associated with the energetic/economic value of the gases produced. This is a main challenge taking into account the complexity of the wastewater depending on its origin. This new application could be of special interest in the case of biomass-derived effluents that are difficult to treat by conventional technologies. In a work closely related to wastewater treatment, Remón *et al.*<sup>15</sup> studied the valorization by APR of whey cheese, containing mainly lactose. The effect of the operating conditions on the yield of gas, liquid and solid by-products was investigated with promising results. The fish-canning industry can be a good candidate since the different production lines generate wastewater with high salinity and variable organic loads that hinder their treatment by biological methods.<sup>16,17</sup>

Studies on the potential application of APR as wastewater treatment are really scarce in the literature. Traditionally, most of the studies on APR are focused on model compounds, providing valuable information of the process, but there are only a few studies on the effect of impurities or mixtures of compounds on the catalyst performance. These studies deal mostly with the APR of crude glycerol in aqueous fractions from biorefineries. Lehnert and Claus<sup>18</sup> reported that the APR of crude glycerol containing NaCl led to a decrease in the  $H_2$  production rate and provoked catalyst deactivation. Boga *et al.*<sup>19</sup> reported that fatty acids, such as stearic and oleic and their salts, long chain alkanes and olefins derived from fatty acids can block partially the Pt active sites of the catalysts supported on different materials in the APR of crude glycerol. Nevertheless, replacing  $Al_2O_3$  by activated carbon as the support significantly improved the glycerol conversion and selectivity to  $H_2$ . King *et al.*<sup>20</sup> assessed the effect of KOH in the APR of glycerol with Pt-Re/C and Pt/C catalysts. The glycerol conversion,  $H_2/CO_2$  ratio and production of aqueous phase oxygenates were increased. Remón *et al.*<sup>21</sup> studied the effect of other bio-diesel impurities such as acetic acid, methanol or KOH in the APR of glycerol with Ni-La/ $Al_2O_3$  catalysts. They reported that the presence of methanol decreased the glycerol conversion, whereas acetic acid and KOH led to decreased and increased gas production, respectively. Remón *et al.*<sup>22</sup> studied the effect of different acids (phosphoric, sulphuric and acetic) and bases (KOH and NaOH) in the APR of glycerol using Ni-La/ $Al_2O_3$  catalysts. They reported that those compounds significantly affect the catalyst deactivation, especially in the case of phosphoric acid and KOH. According to these studies, working with mixtures of compounds can significantly alter the glycerol conversion and selectivity to  $H_2$  obtained in comparison with the results obtained with single species.

The insight into the effect of mixtures of compounds on APR is of special interest when complex matrices such as in-

dustrial wastewater are proposed as substrates in the APR process. In particular, compounds such as acetic and phosphoric acids and sodium chloride are at high concentration in tuna-cooking effluents and can affect the catalyst performance.

The current work presents, for the first time, an exploratory study on the application of APR to the treatment of fish-canning wastewater, using Pt catalysts supported on different carbon materials (two activated carbons and a carbon black). Tuna-cooking effluents were selected due to their significance in the canning industry. Experiments in batch and semi-continuous modes were carried out in order to check the catalyst performance in both reaction systems. The stability of the catalysts was evaluated upon three successive applications.

## 2. Experimental

### 2.1. Materials

Hexachloroplatinic acid solution ( $H_2PtCl_6$ , 8% wt in  $H_2O$ ) and sodium chloride (NaCl, >99%) were purchased from Sigma-Aldrich. Commercial Norit® CAPSUPER (CAPSUPER) and Norit® SXPLUS (SXPLUS) activated carbons were supplied by Cabot Corporation (USA) and ENSACO 350G (ENSACO) carbon black was supplied by TIMCAL Canada Inc. (Canada).

### 2.2. Preparation and characterization of supports and catalysts

The supports were characterized by nitrogen adsorption-desorption isotherms at 77 K (TriStar II, Micromeritics), thermogravimetric analysis (TGA Q500, TA Instruments), elemental analysis (LECO CHNS-932) and slurry pH measurements. The slurry pH was determined by measuring, until a constant value, the pH of an aqueous suspension of the support in distilled water (1 g of solid per 10 mL of water). Pt/C (3%, w) catalysts were prepared by incipient wetness impregnation using two commercial activated carbons (CAPSUPER and SXPLUS) and a carbon black (ENSACO) as supports. Then, they were dried at room temperature for 2 h and introduced in an oven at 333 K overnight. Finally, the catalysts were calcined at 573 K for 2 h and reduced with 30 N mL  $min^{-1}$   $H_2$  flow at 673 K for 2 h. The catalysts were characterized by scanning transmission electron microscopy (JEOL-3000F at 300 kV) and X-ray photoelectron spectroscopy (K-Alpha – Thermo Scientific equipped with an AlKa X-ray excitation source, 1486.68 eV). Software ‘ImageJ 1.44i’ was used for counting and measuring Pt NPs on digital TEM images (more than 200 NPs were measured per catalyst). The mean Pt particle size and standard deviation were calculated. Software ‘XPS peak v4.1’ was used for the deconvolution of the spectrograms in order to obtain the relative occurrence of  $Pt^{2+}$  and  $Pt^0$  species. The data analysis procedure involved smoothing, Shirley background subtraction and mixed Gaussian-Lorentzian by a least-squares method for curve fitting. The C 1s peak (284.6 eV) was used as an internal standard for binding energy corrections due to sample charging.



### 2.3. APR experiments and analytical procedures

Tuna-cooking wastewater was obtained by boiling tuna (*Thunnus alalunga*) in water (0.25 kg tuna per L, 5 g NaCl L<sup>-1</sup>) for 30 min, according to the procedure communicated by a local fish canning industry. The resulting liquor was filtered through 0.45 µm PTFE filters (Scharlab). Experiments were carried out in stainless steel batch reactors (BR100, Berghoff) at 473 K and 24 bar for 4 h, using 0.4 g of catalysts in 20 mL reaction volume under an Ar atmosphere. Semi-continuous experiments were performed by supplying an Ar flow into the reactor (1 N mL min<sup>-1</sup>) using a high pressure flow meter (100 L, Sierra) and a backpressure regulator (Swagelok). The reactors were purged with Ar several times in order to remove the air before runs. The gases were collected in multilayer foil sample bags (Supelco). The aqueous phase was characterized by total organic carbon (TOC) measured in a TOC-VCSH apparatus (Shimadzu), chemical oxygen demand (COD), determined according to the standard method (ASTM D1252), and ion chromatography (883 Basic IC Plus, Metrohm). The gas phase was analyzed with a GC/FID/TCD (7820A, Agilent) using 2 packed columns and a molecular sieve allowing the detection of H<sub>2</sub>, CO, CO<sub>2</sub>, CH<sub>4</sub> and C<sub>2</sub>H<sub>6</sub>.

## 3. Results and discussion

### 3.1. Catalyst and support characterization

Table 1 shows the specific surface area, pore volumes and slurry pH of the supports. All of them showed a high BET surface area, especially the CAPSUPER activated carbon, which also presents a significantly higher contribution of mesoporosity than the SXPLUS one. The ENSACO carbon black was mostly mesoporous but with a fairly high surface area. The slurry pH varied from acidic (CAPSUPER) and slightly acidic (SXPLUS) to basic (ENSACO). The acidic character of CAPSUPER can be attributed to the surface acid groups generated by chemical activation of the carbon. Fig. 1 shows the TEM images and the corresponding size distribution of the Pt NPs. The mean NP size and standard deviation were in the ranges 4.1–11.3 nm and 2.6–8.9 nm, respectively. As shown in the TEM images, the Pt NPs were quite homogeneously dispersed on the carbon supports. XPS characterization yielded Pt<sup>2+</sup>/Pt<sup>0</sup> ratios of 0.5 for the SXPLUS- and ENSACO-supported catalysts, whereas in the case of Pt/CAPSUPER it was as much as 1.5 in spite of the equivalent conditions used in the reduction step. According to the slurry pH and TPD profiles of CAPSUPER,<sup>23</sup> this difference could be related to the occurrence of acid groups on its surface, attracting electrons from Pt.

### 3.2. Characterization of the wastewater

Table 2 shows the TOC and COD values of the starting tuna-cooking wastewater, as well as its pH and the main ionic species. As can be seen, fairly high TOC and COD values were measured (≈1900 and 5000 mg L<sup>-1</sup>, respectively). The COD/TOC ratio (≈2.6) suggests a relative abundance of oxygen-containing organic species, most probably with carboxylic acid groups, consistent with the measured pH value. The five main anions detected corresponded to chloride, acetate, formate, phosphate and sulphate. Chloride was added in the preparation of the tuna-cooking synthetic wastewater, emulating the high salinity medium used in the industrial cooking of tuna. Acetate and formate are short chain fatty acid groups which could come from the breakdown of larger fatty acids upon cooking. Blue fish, such as tuna, is a well-known source of P; hence phosphate was found to be one of the main anionic species. Sulphate was detected at lower concentrations, mainly ascribed to sulphur-containing amino acid degradation.

### 3.3. Aqueous phase reforming runs

**3.3.1 TOC and COD removal.** Fig. 2 shows the TOC and COD removal in the APR experiments carried out with the catalysts and the bare carbon supports in batch and semi-continuous modes. A blank experiment was carried out in the absence of a support, yielding *ca.* 20% TOC and COD removal, which can be partly ascribed to hydrothermal carbonization, since a dark brown solid was recovered by filtration.<sup>24</sup>

The experiments with the bare supports yielded higher TOC and COD removal than the ones with catalysts (55–75% *vs.* 45–60%). As already seen, the carbon supports tested have a high surface area and a porous texture including both micro and mesoporosity. Thus, adsorption of species from the tuna cooking wastewater can represent a main contribution to the disappearance of TOC and COD. Fig. S1 (ESI†) shows the TGA curves under N<sub>2</sub> flow of the supports before and after the APR runs. Differences between the TGA (dTGA) curves for the fresh and used supports can be observed, mainly within the 200–400 °C range, confirming the adsorption onto the carbon materials. However, the TGA curves do not allow the determination of the amount of organic species adsorbed. From the unmatched balance of C, it was estimated that between 80–90% of the TOC removal could be due to adsorption; this represents up to 4–6% of the C weight of the supports. Table S1† shows the elemental analysis of the fresh and used CAPSUPER carbon, which shows a lower relative amount C, and a relatively higher amount of both H

**Table 1** Specific surface area, meso- and micropore volumes and slurry pH of carbon supports

| Support  | BET surface area (m <sup>2</sup> g <sup>-1</sup> ) | Micropore volume (cm <sup>3</sup> g <sup>-1</sup> ) | Mesopore volume (cm <sup>3</sup> g <sup>-1</sup> ) | Slurry pH |
|----------|--|---|--|-----------|
| CAPSUPER | 1750   | 0.66  | 0.63   | 2.6       |
| SXPLUS   | 1210   | 0.53  | 0.38   | 6.5       |
| ENSACO   | 932  | 0.12  | 0.69   | 10.3      |



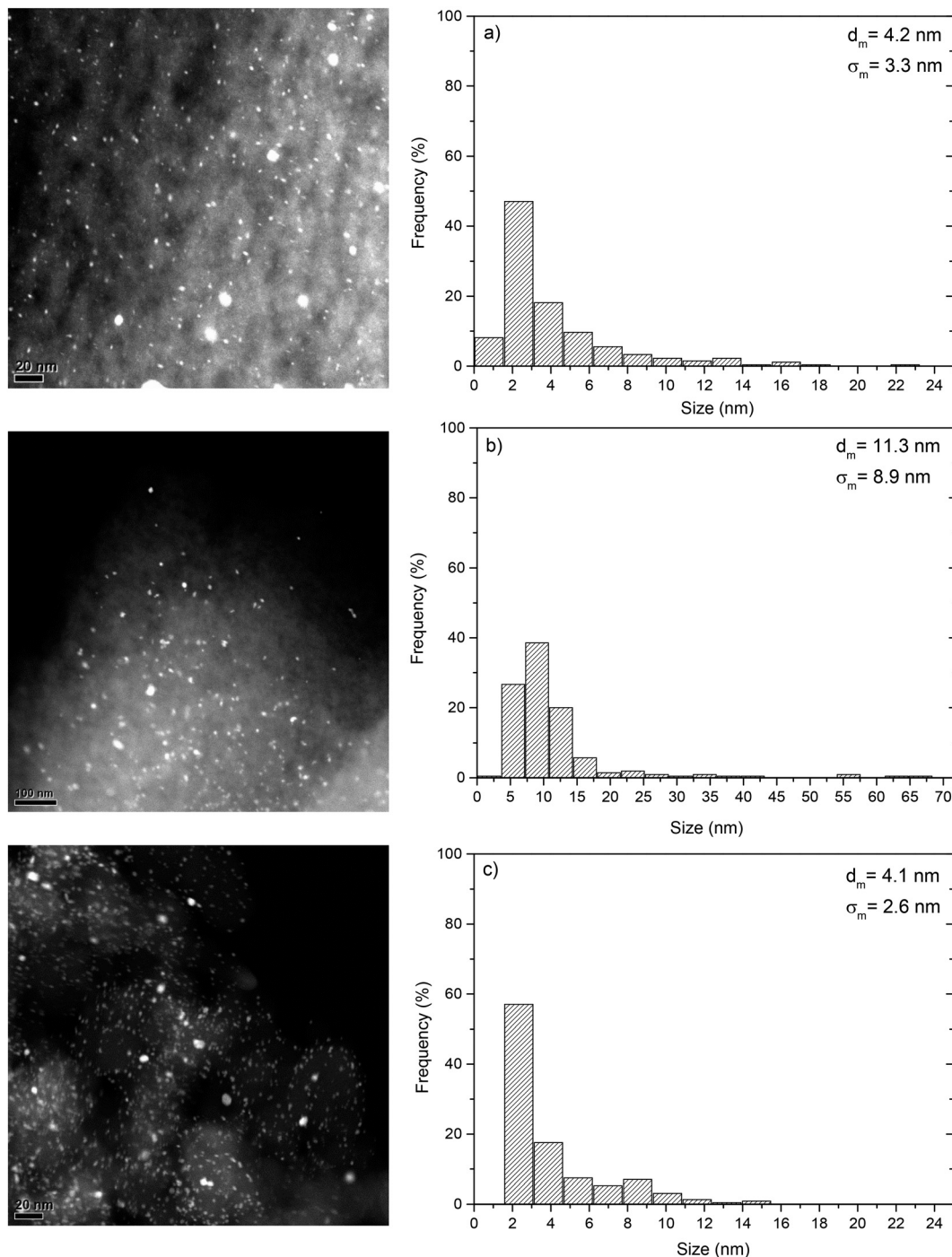


Fig. 1 TEM images of a) Pt/CAPSUPER, b) Pt/SXPLUS and c) Pt/ENSACO.

Table 2 TOC, COD, main anions detected and initial pH of the tuna cooking wastewater

| TOC (mg L <sup>-1</sup> ) | COD (mg L <sup>-1</sup> ) | Chloride (mg L <sup>-1</sup> ) | Acetate (mg L <sup>-1</sup> ) | Formate (mg L <sup>-1</sup> ) | Phosphate (mg L <sup>-1</sup> ) | Sulphate (mg L <sup>-1</sup> ) | Initial pH |
|---------------------------|---------------------------|--------------------------------|-------------------------------|-------------------------------|---------------------------------|--------------------------------|------------|
| 1895 ± 258                | 4996 ± 501                | 3815 ± 219                     | 1895 ± 321                    | 10 ± 9                        | 523 ± 22                        | 16 ± 14                        | 6.1 ± 0.2  |

and N for the used support, consistent with the adsorption of organic species.

Therefore, the main differences in TOC and COD removal in the experiments with the bare supports and the catalysts

can be ascribed mostly to adsorption on the carbon support. The lower removal of TOC and COD with the catalysts can be explained by the reduction of the specific surface area accompanied by Pt impregnation.





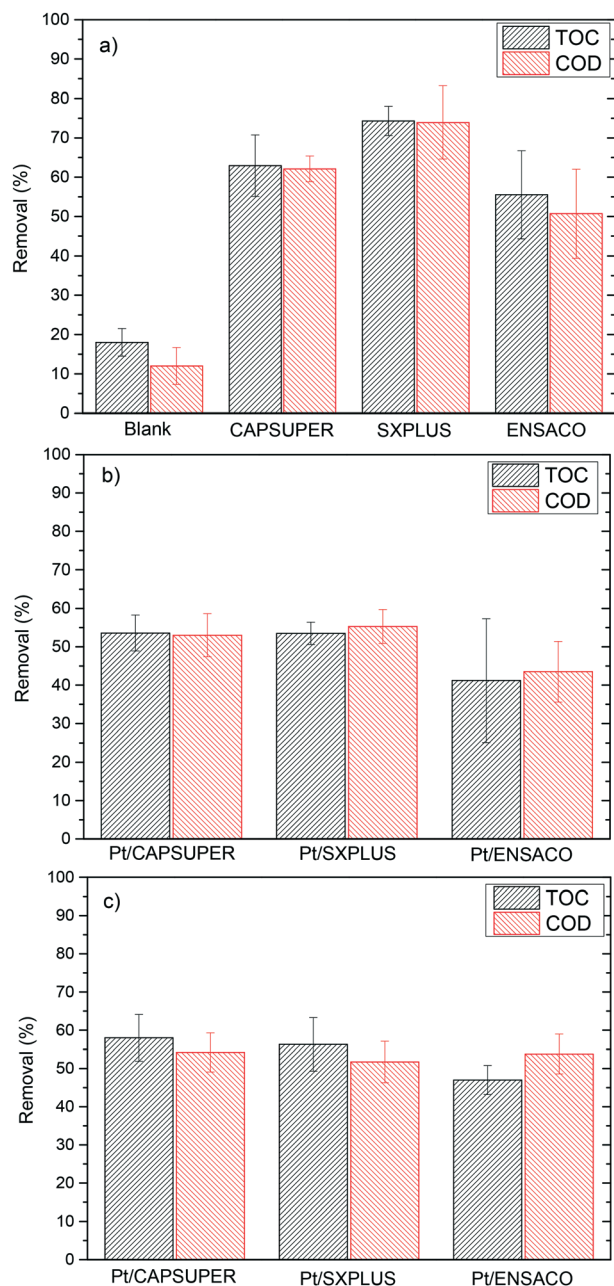


Fig. 2 TOC and COD removal upon APR of tuna-cooking wastewater after 4 h reaction time with a) the carbon supports in batch runs; the Pt/C catalysts b) in batch runs and c) in semi-continuous runs.

**3.3.2 Evolution of the anionic species upon APR.** Fig. 3 depicts the main anionic species detected, excluding chloride, in the initial tuna cooking wastewater and after the APR runs, as analyzed by ion chromatography, acetate was the major component (*ca.* 1900 mg L<sup>-1</sup>) in the initial wastewater and its concentration was barely reduced upon the APR process, indicating its refractory character under the operating conditions tested.<sup>25</sup> Phosphate was found at a much lower concentration than acetate and was not affected by the APR treatment. In the reactions performed with CAPSUPER and Pt/CAPSUPER, the phosphate concentration rose from *ca.*

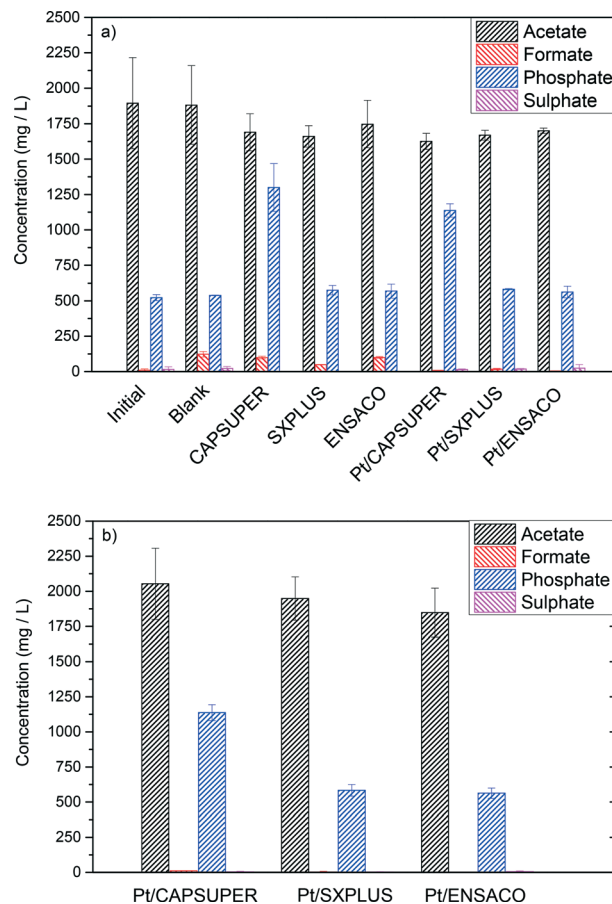


Fig. 3 Evolution of the anionic species upon APR (4 h) with a) supports and catalysts in batch experiments and b) catalysts in semi-continuous runs.

550–600 up to close to 1200 mg L<sup>-1</sup>, which can be ascribed to leaching from the support, which was due to activation with phosphoric acid. Formate was detected at 10 mg L<sup>-1</sup> in the initial tuna cooking wastewater and increased up to over 120 mg L<sup>-1</sup> in the blank experiment. Its concentration reached between 50 and 100 mg L<sup>-1</sup> in the experiments with bare supports, whereas it remained between 5–10 mg L<sup>-1</sup> when the Pt catalysts were used. Formic acid can be produced from glucose conversion upon hydrothermal carbonization through several intermediates such as erythrose, 1,6-anhydro-glucose, hydroxymethylfurfural or lactic acid.<sup>26</sup> This can explain the higher levels of formate in the blank experiment and in those performed with the carbon supports, where HTC must be the main process. With the Pt catalysts, the final formate concentration was lower because formic acid is reformed to CO<sub>2</sub> and H<sub>2</sub> and/or CO and H<sub>2</sub>O. Sulphate concentrations lower than 20 mg L<sup>-1</sup> were found. No significant differences in formate and sulphate concentrations are observed between the batch and semi-continuous operation. Finally, chloride was not significantly affected by the APR treatment.

**3.3.3 Gas phase composition.** Table 3 shows the measured amount of gas under batch and semi-continuous operation, as analyzed by GC. The total amount ranged between 63 and



366  $\mu\text{mol}$ . As indicated in the Experimental section, the experiments were performed with 20 mL of tuna-cooking wastewater, which, according to the starting COD and TOC values, means 100 mg of COD and 38 mg of TOC. The lowest amount was obtained in the blank experiment, while with the bare carbon supports it increased to 123–257  $\mu\text{mol}$ . The carbon black-supported catalyst (Pt/ENSACO) gave the highest gas yield (twice that obtained with the bare support), while the two other catalysts allowed increases only in the semi-continuous experiments. The improved gas yield in this operation mode could be related to gas withdrawal displacing the reaction towards the products.<sup>27</sup> The valuable gases produced significantly increased when the catalysts were used, with Pt/ENSACO showing a production higher than both Pt/CAPSUPER and Pt/SXPLUS.

$\text{H}_2$ ,  $\text{CO}_2$ ,  $\text{CH}_4$  and  $\text{C}_2\text{H}_6$  were the components detected in the gas phase, whereas CO was never detected. Fig. 4 shows the composition of the gas fraction from the batch experiments. The blank run produced mainly  $\text{CO}_2$  (98.4% of the gas fraction) and in a much lower quantity  $\text{H}_2$  (1.3%) and alkanes (0.3%), which can be ascribed to gas products from HTC. With the bare supports,  $\text{CO}_2$  was also by far the major component of the gas fraction (98–99%), with  $\text{H}_2$  (0.4–1.1%) and alkanes (0.1–0.3%) being in a much lower proportion. However, with the catalysts, the  $\text{CO}_2$  percentage slightly decreased (96–97% of the gas fraction) in the case of Pt/CAPSUPER and Pt/SXPLUS. Likewise, the valuable gases ( $\text{H}_2$  and alkanes) increased. The increase of  $\text{H}_2$  percentage of the gas fraction was significant in the case of Pt/CAPSUPER and Pt/ENSACO. With Pt/ENSACO, the  $\text{CO}_2$  percentage decreased (82% of the gas fraction, while  $\text{H}_2$  and alkanes represented 9 and 9%, respectively). The higher activity, in terms of production of gases and  $\text{H}_2$ , of Pt/ENSACO could be partly ascribed to the effect of the basic properties of the support on the catalytic performance. These results are in good agreement with the literature. In this sense, different authors<sup>5,20,28,29</sup> reported that the APR of glycerol was favored in terms of conversion and selectivity to  $\text{H}_2$  with catalysts using basic supports or after addition of KOH to the substrate. Liu *et al.*<sup>29</sup> suggested that basic medium provokes the polarization of  $\text{H}_2\text{O}$  and in-

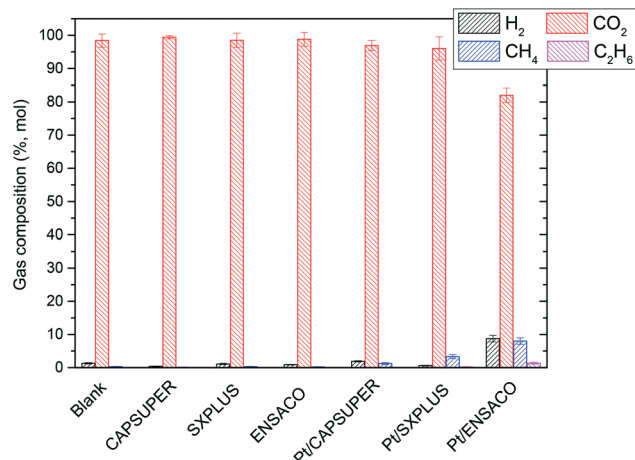


Fig. 4 Composition of the gas fraction from the batch APR experiments.

duces its dissociation and/or directly provides the OH groups to be adsorbed onto the catalysts, which is an important step in the water-gas shift reaction.<sup>30</sup> Likewise, He *et al.*<sup>31</sup> and Liu *et al.*<sup>29</sup> reported that addition of CaO or KOH to the initial biomass solution could *in situ* remove the  $\text{CO}_2$  favoring the water-gas shift reaction by displacing the reaction towards the products and inhibiting methanation reactions. Thus, the basicity of the catalyst in the reaction medium improves the yield of  $\text{H}_2$ , but in some cases at the expense of the gas production. Moreover, some authors pointed out that the absence of Lewis acid surface sites conferring the electronegativity of the support to the metal phase can affect the Pt hydrogenation sites, leading to a low hydrogenation activity and, therefore, a higher  $\text{H}_2$  yield.<sup>13</sup>

Differences were found with the catalysts in semi-continuous runs (Fig. 5). In the cases of Pt/CAPSUPER and Pt/SXPLUS, the alkane percentage decreased compared to that in the batch experiments (from 1.3% to 0.3% and from 3.5% to 2.0% of the gas fraction, respectively). With Pt/ENSACO, the resulting gas was also less rich in  $\text{H}_2$  (from 9% to 4.5%) while the  $\text{CO}_2$  percentage increased from 82% to

Table 3 Amount of gas produced and C conversion to detected gases in the APR experiments

| Catalysts   | Operation mode  | Total detected gas ( $\mu\text{mol}$ ) | Valuable gases ( $\text{H}_2$ + alkanes, $\mu\text{mol}$ ) | C conversion to detected gases (%) |
|-------------|-----------------|--|--|------------------------------------|
| Blank       |                 | 63 $\pm$ 10                            | 1.0 $\pm$ 1.0  | 2 $\pm$ 1                          |
| CAPSUPER    |                 | 257 $\pm$ 32                           | 1.4 $\pm$ 1.0  | 8 $\pm$ 1                          |
| SXPLUS      |                 | 174 $\pm$ 27                           | 2.6 $\pm$ 1.0  | 5 $\pm$ 1                          |
| ENSACO      | Batch           | 124 $\pm$ 8                            | 1.4 $\pm$ 1.0  | 4 $\pm$ 1                          |
| Pt/CAPSUPER |                 | 173 $\pm$ 25                           | 5.4 $\pm$ 1.0  | 5 $\pm$ 1                          |
| Pt/SXPLUS   |                 | 158 $\pm$ 18                           | 6.3 $\pm$ 1.0  | 5 $\pm$ 1                          |
| Pt/ENSACO   |                 | 268 $\pm$ 35                           | 48.3 $\pm$ 5.0   | 8 $\pm$ 1                          |
| Pt/CAPSUPER |                 | 279 $\pm$ 35                           | 6.6 $\pm$ 1.0  | 8 $\pm$ 1                          |
| Pt/SXPLUS   | Semi-continuous | 229 $\pm$ 37                           | 6.1 $\pm$ 1.0  | 6 $\pm$ 1                          |
| Pt/ENSACO   |                 | 366 $\pm$ 47                           | 47.8 $\pm$ 6.0   | 10 $\pm$ 1                         |

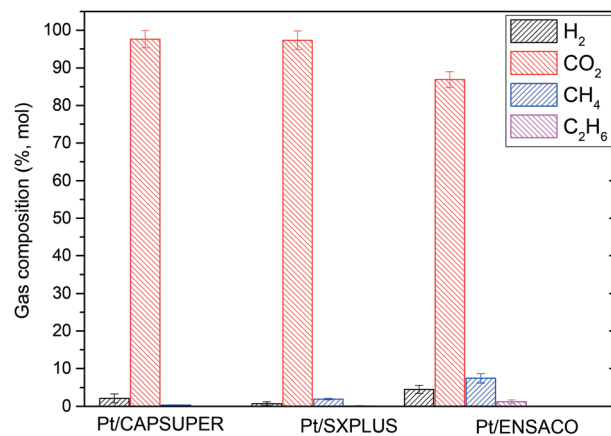


Fig. 5 Composition of the gas fraction from the semi-continuous APR experiments.



**Table 4** Gas production with the catalysts tested upon 3 successive runs

| Catalysts   | Total gas<br>( $\mu\text{mol}$ ) | Gas composition (mol, %) |                 |                 |                               |
|-------------|----------------------------------|--------------------------|-----------------|-----------------|-------------------------------|
|             |                                  | H <sub>2</sub>           | CO <sub>2</sub> | CH <sub>4</sub> | C <sub>2</sub> H <sub>6</sub> |
| Pt/CAPSUPER |                                  |                          |                 |                 |                               |
| Cycle #1    | 173 $\pm$ 25                     | 1.8 $\pm$ 0.2            | 96.9 $\pm$ 1.5  | 1.2 $\pm$ 0.2   | 0.10 $\pm$ 0.05               |
| Cycle #2    | 220 $\pm$ 54                     | 1.2 $\pm$ 0.4            | 98.3 $\pm$ 1.3  | 0.5 $\pm$ 0.2   | 0                             |
| Cycle #3    | 150 $\pm$ 20                     | 1.5 $\pm$ 0.2            | 98.2 $\pm$ 1.6  | 0.3 $\pm$ 0.2   | 0                             |
| Pt/SXPLUS   |                                  |                          |                 |                 |                               |
| Cycle #1    | 158 $\pm$ 18                     | 0.5 $\pm$ 0.2            | 96.0 $\pm$ 3.5  | 3.3 $\pm$ 0.6   | 0.2 $\pm$ 0.1                 |
| Cycle #2    | 200 $\pm$ 47                     | 2.7 $\pm$ 0.3            | 96.2 $\pm$ 3.3  | 1.1 $\pm$ 0.2   | 0                             |
| Cycle #3    | 120 $\pm$ 37                     | 4.2 $\pm$ 0.3            | 95.4 $\pm$ 3.6  | 0.4 $\pm$ 0.1   | 0                             |
| Pt/ENSACO   |                                  |                          |                 |                 |                               |
| Cycle #1    | 268 $\pm$ 35                     | 8.7 $\pm$ 1.6            | 82.0 $\pm$ 2.0  | 8 $\pm$ 0.8     | 1.3 $\pm$ 0.3                 |
| Cycle #2    | 230 $\pm$ 39                     | 6.3 $\pm$ 1.5            | 86.7 $\pm$ 1.8  | 6.2 $\pm$ 0.7   | 0.8 $\pm$ 0.2                 |
| Cycle #3    | 190 $\pm$ 25                     | 12.9 $\pm$ 2.0           | 84.8 $\pm$ 2.2  | 2.2 $\pm$ 0.3   | 0.10 $\pm$ 0.05               |

87% and that of alkanes remained almost similar ( $\approx 9\%$ ). In the semi-continuous experiments, part of the gas phase is withdrawn during the reaction, displacing the reaction towards the products. Nevertheless, the total amount of valuable gases did not vary significantly except for Pt/CAPSUPER, where the semi-continuous experiments yielded 6.6  $\mu\text{mol}$  vs. 5.4  $\mu\text{mol}$  in batch mode. Likewise, since the amount of gas products in the reactor is lower, side reactions consuming H<sub>2</sub>, such as the methanation, Fischer-Tropsch, dehydration and hydrogenation reactions, are hindered. This could explain the lower alkane percentage in the case of Pt/CAPSUPER and Pt/SXPLUS. However, in the case of Pt/ENSACO, the lower H<sub>2</sub> and the higher CO<sub>2</sub> percentage compared to the batch experiments, suggests that the water gas shift reaction is also favored while those giving rise to alkanes do not seem to be hindered. This is in good agreement with Guo *et al.*<sup>28</sup> who reported that the basic sites are preferred for the water gas shift reaction and further increased the APR.

**3.3.4 Catalyst stability.** The catalysts were used in three successive applications in batch mode. TOC and COD removal ranged between 20–30% after the three successive uses, but no significant changes were found with regard to

the anionic species. The results on the amount and composition of the gas fraction are summarized in Table 4. The total amount of gases produced did not vary upon the successive runs in the case of Pt/CAPSUPER and Pt/SXPLUS, whereas in the case of Pt/ENSACO it decreased from 268 to 190  $\mu\text{mol}$ . This deactivation can be provoked by acetic and phosphoric acids or by chloride, which are at higher concentrations in the reaction medium and have been recognized as deactivating species in the APR of crude glycerol.<sup>18,22</sup> Their effects can be better observed with the more active catalysts, since Pt/CAPSUPER and Pt/SXPLUS did not show significant differences in the amount of gases produced compared with the bare supports. The H<sub>2</sub> percentage remained unchanged in the case of Pt/CAPSUPER after the 3 successive runs, whereas in the case of Pt/SXPLUS and Pt/ENSACO it significantly increased. Meanwhile, the alkane percentage significantly decreased in all the cases. Table 5 shows the Pt NP mean size, Pt<sup>2+</sup>/Pt<sup>0</sup> ratio and specific surface area of the catalysts after the 3 successive runs. Table 5 also shows the initial slurry pH values, which are not significantly different compared to those of the starting supports. The Pt NP mean size increased with the number of runs due to sintering. However, in the case of Pt/ENSACO there were no significant differences in nanoparticle size after the first use, but after the 3 runs, Pt/ENSACO showed a significantly lower mean size and standard deviation than Pt/CAPSUPER and Pt/SXPLUS. Thus, Pt/ENSACO showed a higher resistance to NP sintering. The increase in H<sub>2</sub> and the decrease in alkane percentages can be explained by the lower number of low-coordinated Pt sites, promoting methanation reactions, as the Pt NP size increases.<sup>32</sup>

Small changes in the Pt<sup>2+</sup>/Pt<sup>0</sup> ratio along the cycles were observed, except for Pt/CAPSUPER, where that ratio significantly decreased after the first use, showing the influence of the support. The specific surface of the catalysts decreased upon the 3 successive uses probably due to the adsorption of organic species, condensation and/or carbon formation. Table 6 shows the atomic percentage of some elements of interest in the catalyst surface as obtained by XPS after each

**Table 5** Pt NP mean size, Pt<sup>2+</sup>/Pt<sup>0</sup> ratio and specific surface area of the catalysts tested upon 3 successive runs

| Catalysts      | Size (nm)       | Pt <sup>2+</sup> /Pt <sup>0</sup> ratio | Specific surface area (m <sup>2</sup> g <sup>-1</sup> ) | pH slurry |
|----------------|-----------------|---|---|-----------|
| Pt/CAPSUPER    |                 |   |   |           |
| Initial        | 4.2 $\pm$ 3.3   | 1.5                                     | 1687  | 2.9       |
| After cycle #1 | 8.8 $\pm$ 6.9   | 1.0                                     |   |           |
| After cycle #2 | 13.4 $\pm$ 12.0 |   | 1160  |           |
| After cycle #3 | 27.8 $\pm$ 56.9 | 1.2                                     |   |           |
| Pt/SXPLUS      |                 |   |   |           |
| Initial        | 11.3 $\pm$ 8.9  | 0.5                                     | 1040  | 7.0       |
| After cycle #1 |                 |   |   |           |
| After cycle #2 | 17.6 $\pm$ 24.9 | 0.7                                     | 454   |           |
| After cycle #3 | 26.3 $\pm$ 45.2 | 0.7                                     |   |           |
| Pt/ENSACO      |                 |   |   |           |
| Initial        | 4.1 $\pm$ 2.6   | 0.5                                     | 678   | 9.9       |
| After cycle #1 | 3.8 $\pm$ 2.7   | 0.3                                     |   |           |
| After cycle #2 |                 |   | 401   |           |
| After cycle #3 | 14.6 $\pm$ 18.9 | 0.5                                     |   |           |





**Table 6** Atomic percentage of selected elements in the catalyst surface as obtained by XPS

| Catalysts      | C (%) | O (%) | N (%) | Na (%) | P (%) | Cl (%) |
|----------------|-------|-------|-------|--------|-------|--------|
| Pt/CAPSUPER    |       |       |       |        |       |        |
| Initial        | 92.0  | 6.8   | 0     | 0.1    | 1.0   | 0      |
| After cycle #1 | 91.2  | 6.8   | 2.0   | 0.2    | 0.4   | 0      |
| After cycle #2 | 88.8  | 6.8   | 2.8   | 0.3    | 0.5   | 0      |
| After cycle #3 | 87.6  | 6.7   | 3.6   | 0.3    | 0.6   | 0      |
| Pt/SXPLUS      |       |       |       |        |       |        |
| Initial        | 96.6  | 3.2   | 0     | 0      | 0     | 0      |
| After cycle #1 | 93.5  | 3.7   | 1.8   | 0.2    | 0     | 0.1    |
| After cycle #2 | 90.8  | 4.6   | 2.5   | 0.2    | 0.2   | 0.1    |
| After cycle #3 | 88.8  | 6.8   | 2.9   | 0.3    | 0.5   | 0.1    |
| Pt/ENSACO      |       |       |       |        |       |        |
| Initial        | 98.5  | 1.1   | 0     | 0      | 0     | 0      |
| After cycle #1 | 96.1  | 1.8   | 1.2   | 0.3    | 0     | 0.5    |
| After cycle #2 | —     | —     | —     | —      | —     | —      |
| After cycle #3 | 94.8  | 2.3   | 2.1   | 0.3    | 0     | 0.5    |

cycle of use. The relative abundance of the major element (C) decreased while that of N increased with the number of runs, probably due to the adsorption of N-containing compounds, such as amino-acids. In the case of Pt/CAPSUPER, the relative amount of O did not vary after the 3 successive runs, whereas in Pt/SXPLUS and Pt/ENSACO it increased. Interestingly, the surface concentration of Na increased in the three catalysts up to 0.3%. Boga *et al.*<sup>19</sup> found that Na salts of fatty acids greatly inhibited the activity of Pt/Al<sub>2</sub>O<sub>3</sub> (1% wt) catalysts in the APR of the synthetic crude glycerol effluent, decreasing the selectivity to H<sub>2</sub>. Thus, the presence of Na may have a role in the decreased performance of our catalysts upon use. Phosphorous was found mainly in Pt/CAPSUPER and to a less extent in Pt/SXPLUS, but not in the case of Pt/ENSACO. On the contrary, Cl was at a higher concentration in Pt/ENSACO and Pt/SXPLUS. Mostany *et al.*<sup>33</sup> performed thermodynamics studies of phosphate adsorption on the Pt surface in acid medium, reporting a stronger interaction of adsorbed phosphate species with Pt, even higher than in the case of sulphate. Likewise, the adsorption of P species can prevent CO adsorption on Pt,<sup>34</sup> hindering the water-gas shift reaction.

Due to the complex matrix of the wastewater, from the results in this work it is not possible to ascribe to individual compounds contributions to catalyst deactivation. Besides, deactivation takes place also due to the contribution of hydrothermal carbonization and aging of the metal phase due to hydrothermal treatment. However, tuning of catalyst properties according to the nature of the reaction medium is needed to prevent deactivation, which deserves future research work.

## 4. Conclusions

An exploratory study on APR of tuna-cooking wastewater was performed at 473 K and 24 bar using Pt catalysts (3% wt) supported on different carbon materials (two activated carbons and a carbon black) for the first time. Hydrothermal carbonization (20% of TOC and COD removal) was observed

when the reactions were carried out without supports/catalysts in the reaction medium. The carbon supports adsorbed tuna-cooking wastewater components (up to 90% of TOC removal) and also promoted the production of gases, although carbon dioxide was the predominant gas component. With the catalysts, the percentage of valuable gases (hydrogen and alkanes) increased significantly, reaching up to 18% of the gas fraction. However, the total amount of gas produced was low (366  $\mu$ mol from a starting 20 mL wastewater volume with 100 mg of COD) probably due to the presence of large amounts of acetic and phosphoric acids as well as chloride ions leading to catalyst deactivation. With the catalyst supported on carbon black, having a basic character, the total amount of gas as well as the percentage of valuable components (H<sub>2</sub> and light alkanes) increased significantly. The type of reaction system affected the production of gases, with the semi-continuous runs yielding a higher amount of gas, since the withdrawn gas displaces the reaction towards the products. As a general trend, the percentage of alkanes and H<sub>2</sub> decreased and increased, respectively, upon 3 successive runs. This could be ascribed to the decreasing number of low-coordinated Pt sites (responsible for methanation) as the size of Pt NPs increased.

## Conflicts of interest

None.

## Acknowledgements

The authors greatly appreciate financial support from Spanish MINECO (CTQ2015-65491-R). A. S. Oliveira thanks the Spanish MINECO for a research grant (BES-2016-077244).

## References

- 1 R. D. Cortright, R. R. Davda and J. A. Dumesic, Hydrogen from Catalytic Reforming of Biomass-derived Hydrocarbons in Liquid Water, *Nature*, 2002, **418**, 964–967.
- 2 R. R. Davda, R. Alcalá, J. Shabaker, G. Huber, R. D. Cortright, M. Mavrikakis and J. A. Dumesic, DFT and Experimental Studies of C-C and C-O Bond Cleavage in Ethanol and Ethylene Glycol on Pt Catalysts, *Stud. Surf. Sci. Catal.*, 2003, **145**, 79–84.
- 3 R. R. Davda and J. A. Dumesic, Renewable Hydrogen by Aqueous-phase Reforming of Glucose, *Chem. Commun.*, 2004, 36–37.
- 4 J. W. Shabaker, R. R. Davda, G. W. Huber, R. D. Cortright and J. A. Dumesic, Aqueous-Phase Reforming of Methanol and Ethylene Glycol Over Alumina-Supported Platinum Catalysts, *J. Catal.*, 2003, **215**, 344–352.
- 5 G. Wen, Y. Xu, H. Ma, Z. Xu and Z. Tian, Production of Hydrogen by Aqueous-Phase Reforming of Glycerol, *Int. J. Hydrogen Energy*, 2008, **33**, 6657–6666.
- 6 Y. Wei, H. Lei, Y. Liu, L. Wang, L. Zhu, X. Zhang, G. Yadavalli, B. Ahring and S. Chen, Renewable Hydrogen Produced from Different Renewable Feedstock by Aqueous-





- Phase Reforming Process, *J. Sustainable Bioenergy Syst.*, 2014, 4(2), 15–21.
- 7 A. V. Kirilin, A. V. Tokarev, L. M. Kustov, T. Salmi, J. Mikkola and D. Y. Murzin, Aqueous Phase Reforming of Xylitol and Sorbitol: Comparison and Influence of Substrate Structure, *Appl. Catal., A*, 2012, 435, 172–180.
  - 8 L. I. Godina, A. V. Kirilin, A. V. Tokarev and D. Y. Murzin, Aqueous Phase Reforming of Industrially Relevant Sugar Alcohols with Different Chiralities, *ACS Catal.*, 2015, 5, 2989–3005.
  - 9 T. Nozawa, Y. Mizukoshi, A. Yoshida and S. Naito, Aqueous Phase Reforming of Ethanol and Acetic Acid Over TiO<sub>2</sub> Supported Ru Catalysts, *Appl. Catal., B*, 2014, 146, 221–226.
  - 10 K. Koichumanova, A. K. K. Vikla, D. J. M. de Vlieger, K. Seshan, B. L. Mojet and L. Lefferts, Towards Stable Catalysts for Aqueous Phase Conversion of Ethylene Glycol for Renewable Hydrogen, *ChemSusChem*, 2013, 6, 1717–1723.
  - 11 A. Seretis and P. Tsiakaras, Aqueous Phase Reforming (APR) of Glycerol Over Platinum Supported on Al<sub>2</sub>O<sub>3</sub> Catalyst, *Renewable Energy*, 2016, 85, 1116–1126.
  - 12 N. D. Subramanian, J. Callison, C. R. A. Catlow, P. P. Wells and N. Dimitratos, Optimised Hydrogen Production by Aqueous Phase Reforming of Glycerol on Pt/Al<sub>2</sub>O<sub>3</sub>, *Int. J. Hydrogen Energy*, 2016, 41, 18441–18450.
  - 13 A. Ciftci, B. Peng, A. Jentys, J. A. Lercher and E. J. M. Hensen, Support Effects in the Aqueous Phase Reforming of Glycerol Over Supported Platinum Catalysts, *Appl. Catal., A*, 2012, 431, 113–119.
  - 14 A. Ciftci, D. A. J. M. Ligthart and E. J. M. Hensen, Aqueous phase reforming of glycerol over Re-promoted Pt and Rh catalysts, *Green Chem.*, 2014, 853–863.
  - 15 J. Remón, L. García and J. Arauzo, Cheese Whey Management by Catalytic Steam Reforming and Aqueous Phase Reforming, *Fuel Process. Technol.*, 2016, 154, 66–81.
  - 16 J. Zufia and G. Aurrekoetxea, Integrated Processing of Fish Canning Industry Wastewater, *J. Aquat. Food Prod. Technol.*, 2002, 11, 303–315.
  - 17 S. Muthukumaran and K. Baskaran, Organic and Nutrient Reduction in a Fish Processing Facility – A Case Study, *Int. Biodeterior. Biodegrad.*, 2013, 85, 563–570.
  - 18 K. Lehnert and P. Claus, Influence of Pt Particle Size and Support Type on the Aqueous-Phase Reforming of Glycerol, *Catal. Commun.*, 2008, 9, 2543–2546.
  - 19 D. A. Boga, F. Liu, P. C. A. Bruijninx and B. M. Weckhuysen, Aqueous-phase reforming of crude glycerol: effect of impurities on hydrogen production, *Catal.: Sci. Technol.*, 2016, 6, 134–143.
  - 20 D. L. King, L. Zhang, G. Xia, A. M. Karim, D. J. Heldebrant, X. Wang, T. Peterson and Y. Wang, Aqueous Phase Reforming of Glycerol for Hydrogen Production Over Pt-Re Supported on Carbon, *Appl. Catal., B*, 2010, 99, 206–213.
  - 21 J. Remón, J. Ruiz, M. Oliva, L. García and J. Arauzo, Effect of Biodiesel-Derived Impurities (Acetic Acid, Methanol and Potassium Hydroxide) on the Aqueous Phase Reforming of Glycerol, *Chem. Eng. J.*, 2016, 299, 431–448.
  - 22 J. Remón, C. Jarauta-Córdoba, L. García and J. Arauzo, Effect of Acid (CH<sub>3</sub>COOH, H<sub>2</sub>SO<sub>4</sub> and H<sub>3</sub>PO<sub>4</sub>) and Basic (KOH and NaOH) Impurities on Glycerol Valorisation by Aqueous Phase Reforming, *Appl. Catal., B*, 2017, 219, 362–371.
  - 23 J. Lemus, J. Palomar, M. A. Gilarranz and J. J. Rodriguez, On the Kinetics of Ionic Liquid Adsorption onto Activated Carbons from Aqueous Solution, *Ind. Eng. Chem. Res.*, 2013, 52, 2969–2976.
  - 24 J. Fang, L. Zhan, Y. S. Ok and B. Gao, Minireview of Potential Applications of Hydrochar Derived from Hydrothermal Carbonization of Biomass, *J. Ind. Eng. Chem.*, 2018, 57, 15–21.
  - 25 D. J. M. de Vlieger, D. B. Thakur, L. Lefferts and K. Seshan, Carbon Nanotubes: A Promising Catalyst Support Material for Supercritical Water Gasification of Biomass Waste, *ChemCatChem*, 2012, 4, 2068–2074.
  - 26 X. Lu, J. R. V. Flora and N. D. Berge, Influence of Process Water Quality on Hydrothermal Carbonization of Cellulose, *Bioresour. Technol.*, 2014, 154, 229–239.
  - 27 I. Coronado, M. Stekrova, M. Reinikainen, P. Simell, L. Lefferts and J. Lehtonen, A Review of Catalytic Aqueous-Phase Reforming of Oxygenated Hydrocarbons Derived from Biorefinery Water Fractions, *Int. J. Hydrogen Energy*, 2016, 41, 11003–11032.
  - 28 Y. Guo, M. U. Azmat, X. Liu, Y. Wang and G. Lu, Effect of support's Basic Properties on Hydrogen Production in Aqueous-Phase Reforming of Glycerol and Correlation between WGS and APR, *Appl. Energy*, 2012, 92, 218–223.
  - 29 J. Liu, X. Chu, L. Zhu, J. Hu, R. Dai, S. Xie, Y. Pei, S. Yan, M. Qiao and K. Fan, Simultaneous Aqueous-Phase Reforming and KOH Carbonation to Produce CO<sub>x</sub>-Free Hydrogen in a Single Reactor, *ChemSusChem*, 2010, 3, 803–806.
  - 30 R. He, R. R. Davda and J. A. Dumesic, In Situ ATR-IR Spectroscopic and Reaction Kinetics Studies of Water-Gas Shift and Methanol Reforming on Pt/Al<sub>2</sub>O<sub>3</sub> Catalysts in Vapor and Liquid Phases, *J. Phys. Chem. B*, 2005, 109, 2810–2820.
  - 31 C. He, J. Zheng, K. Wang, H. Lin, J. Wang and Y. Yang, Sorption Enhanced Aqueous Phase Reforming of Glycerol for Hydrogen Production Over Pt-Ni Supported on Multi-Walled Carbon Nanotubes, *Appl. Catal., B*, 2015, 162, 401–411.
  - 32 M. P. Andersson, F. Abild-Pedersen, I. N. Remediakis, T. Bligaard, G. Jones, J. Engbæk, O. Lytken, S. Horch, J. H. Nielsen, J. Sehested, J. R. Rostrup-Nielsen, J. K. Nørskov and I. Chorkendorff, Structure Sensitivity of the Methanation Reaction: H<sub>2</sub>-Induced CO Dissociation on Nickel Surfaces, *J. Catal.*, 2008, 255, 6–19.
  - 33 J. Mostany, P. Martínez, V. Climent, E. Herrero and J. M. Feliu, Thermodynamic Studies of Phosphate Adsorption on Pt(111) Electrode Surfaces in Perchloric Acid Solutions, *Electrochim. Acta*, 2009, 54, 5836–5843.
  - 34 O. Heikkinen, H. Pinto, G. Sinha, S. K. Hämäläinen, J. Sainio, S. Öberg, P. R. Briddon, A. S. Foster and J. Lahtinen, Characterization of a Hexagonal Phosphorus Adlayer on Platinum (111), *J. Phys. Chem. C*, 2015, 119, 12291–12297.

